Joining analysis of polypropylene parts in rotary friction welding process and developing of joints profile

Döner sürtünmeli kaynak işleminde polipropilen parçaların birleşim analizi ve birleşme profilinin geliştirmesi

Yazar(lar) (Author(s)): Hakan MADEN[1], Kerim ÇETİNKAYA[2]

*ORCID[1]: 0000-0002-0912-7310*

ORCID[2]: 0000-0001-9537-1821

Joining Analysis of Polypropylene Parts in Rotary Friction Welding Process and Developing of Joints Profile

Highlight

❖ *Investigation of plastic friction welding nozzles used in production*

❖ *Identifying the problem occurring in plastic parts after rotary friction welding*

❖ *Making data entries for analysis in the current semi-melted state ABAQUS program*

❖ *Analysis and simulations in the current semi-melted state ABAQUS to obtain data*

❖ *Semi-melt agglomeration confinement of the developed structure by making Abaqus analysis and simulations.*

Graphical Abstract

Rotating friction welding is used in the assembly of inline filters. After this welding, semi-melted agglomerations occur on the inner and outer parts. In order to prevent these accumulations, analyzes have been made in the ABAQUS program and the current situation has been obtained. Later, the weld nozzle design was changed and analyzes were made and semi-melt agglomeration was confined.
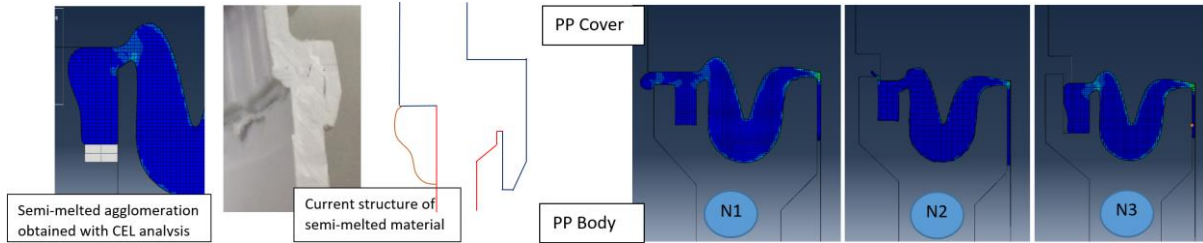
Figure. Confinement of semi-melt build-up after rotary friction welding

Aim

Development of the weld nozzle profile that will contain the semi-melt agglomeration that will occur in the interior after rotary friction welding of plastic parts.

Design & Methodology

Welding nozzle design is made in modules in ABAQUS program. The design was developed by the parameters entered and the interpretation of the analysis results made in the ABAQUS program.

Originality

The source mouth obtained as a result of the ABAQUS program reveals the originality of this study. In addition, with the rotary friction welding simulation, graphs such as temperature, stress and displacement occurred during welding were created.

Findings

With this study, a structure that will contain the semi-melt agglomeration has been obtained as a result of rotary friction welding. During welding, for a piece max. 166,2 °C, 1,9 mm displacement and max. the stress was found to be 4,9253MPa.

Conclusion

As a result of 3 different welding nozzle designs and analysis made to include semi-melt agglomeration, it was observed that the design number 3 imprisoned the melt agglomeration.

Declaration of Ethical Standards

Bu makalenin yazar(lar)ı çalışmalarında kullandıkları materyal ve yöntemlerin etik kurul izni ve/veya yasal-özel bir izin gerektirmediğini beyan ederler. / The author(s) of this article declare that the materials and methods used in this study do not require ethical committee permission and/or legal-special permission.

Joining Analysis of Polypropylene Parts in Rotary Friction Welding Process and Developing of Joints Profile

Araştırma Makalesi / Research Article

Hakan MADEN[1*], Kerim ÇETİNKAYA[2]

[1]İhlas Ev Aletleri İmalat Sanayi ve Ticaret A.Ş., İstanbul/ TURKEY
[2]Antalya AKEV University, Faculty of Art and Design, Antalya, Turkey

ABSTRACT

Various welding methods are used to produce non-detachable joints of plastic parts. These are friction welding (FW), friction-stir welding (FSW), ultrasonic welding, chemical bonding, and hot plate welding. Rotary friction welding (RFW) method, which is one of the FW methods, is generally used in joining the filter parts of water treatment devices. After RFW processes, semi-melted plastic accumulations tend to occur on the interior surfaces of the filter parts. In some cases, particles broken off from these accumulations can often clog sensitive filters. In this study, it is aimed to develop a welding joint profile design that can be used to confine the semi-melted agglomeration formed in the interior surfaces of the filter parts. For this purpose, the semi-melted agglomeration in the filter parts is analyzed/simulated utilizing the ABAQUS program by using Lagrangian and CEL (Coupled Eulerian-Lagrangian) methods, and their thermal analysis, stress, and energy data are evaluated. The analysis is repeated until the optimal welding structure design to confine the semi-melted agglomeration is developed. As a result of the analyses, it was determined that the maximum temperature reached is 166.2 °C, there was a 1.98 mm shortening in the length of the product after welding, and the temperature of 150 °C was reached in 13.1 milliseconds. From the several joint profile designs proposed, it was determined that the N3 joint profile design accommodates the semi-melt raw material better than the others.

Keywords: Rotating friction welding, ABAQUS, CEL analysis, semi-melted agglomeration analysis, joint profile design.

Döner Sürtünmeli Kaynak İşleminde Polipropilen Parçaların Birleşim Analizi ve Birleştirme Profilinin Geliştirilmesi

ÖZ

Plastik parçaların sökülemeyen birleştirmelerinde sürtünme kaynak, sürtünme-karıştırma kaynak, ultrasonik kaynak, kimyasal birleştirme, sıcak plaka kaynak gibi yöntemler kullanılmaktadır. Su arıtma cihazlarının filtre parçaların birleştirilmesinde çoğunlukla sürtünme kaynak yöntemlerinden döner sürtünme kaynağı kullanılmaktadır. Filtre parçalarının döner sürtünme kaynak sonrası iç kısımlarda yarı ergimiş yığılmalar oluşmaktadır. Bazı hassas filtrelerde iç kısımda oluşan yarı ergimiş yığılmalarda kopmalar sonucunda filtrelerin tıkanmasına sebep olmaktadır. Bu çalışmada filtre parçalarının iç kısımda oluşan yarı ergimiş yığılmayı hapsetmek için kaynak ağız tasarımının geliştirilmesi amaçlanmaktadır. Bu amaçla mevcut filtre parçalarının yarı ergimiş yığılma durumu ABAQUS programında (Lagrangian ve CEL (Coupled Eulerian Labrangian) yöntem) analiz/simülasyonlar yaparak yarı ergimiş yığılma durumu, termal analiz, stress, enerji verileri değerlendirilmiştir. Yarı ergimiş yığılma hapsedecek kaynak yapı tasarımı geliştirilerek, analizler tekrarlanmıştır. Elde edilen analizlerde; maksimum sıcaklığın 166,2 °C, kaynak sonrası ürün boyunda 1,98 mm kısalma olduğu ve 150 °C sıcaklığa 13,1 salisede ulaştığı bulunmuştur. Önerilen farklı kaynak ağızları çalışmalarından, N3 kaynak ağızının yarı ergiyik durumdaki hammaddeyi hapsetmesini daha iyi başarım sergilediği tespit edilmiştir.

Anahtar kelime: Döner sürtünmeli kaynak, ABAQUS, CEL analiz, yarı ergimiş yığılma analizi, kaynak ağız profil tasarımı

1. INTRODUCTION

FW is a class of solid-state welding processes. FW occurs by converting mechanical energy into heat energy by friction between the joining surfaces of the parts to be welded and by applying pressure to these parts along their axes. According to this definition, both pressures are applied and heat is created during a FW [1-4]. In the RFW method, usually one of the parts is rotating while the other is stationary. The welding method is shown schematically in figure 1. When the rotation speed reaches a certain level, the two parts are brought into

Sorumlu Yazar (Corresponding Author)
*e-posta : hakanmaden74@gmail.com

contact with each other. This is called front contact. After the front contact, axial pressure is applied to heat the parts. In this stage, the material comes out of the heated area in a semi-melted form. In RFW, generally, the first movement is the rotational movement and the second movement is the axial movement [5].
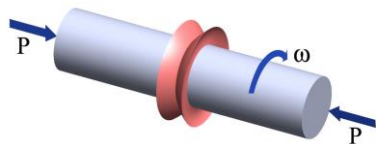

Figure 1. Rotational friction welding [6]

The FSW (Friction Stir Welding) method is a joining technique that is developed for easy and problem-free joining of aluminum alloys and its applications in the industry have become widespread. Yan et al. [8] successfully combined AA6061-T6 aluminum plate and GFR (Glass Fiber Reinforced) nylon filler material using FSW technology to combine aluminum alloy and GFR nylon sheets. They studied the effects of rotational speed, immersion depth, and weld speed on joint morphology, mechanical properties, and part geometry in detail.

Xu et al. [9] successfully joined 1045 carbon steel and 30CrMnSiNi2A high strength low alloy (HSLA) steel by using RFW. The effects of rotation speed on the microstructure and mechanical properties of the weld zone are also analyzed. With increasing rotation speed, tensile strength first increased and then decreased. They found that the highest tensile strength (713 MPa), the greatest elongation (15.3%), and the highest impact toughness (28.8 J/cm2) are achieved at a rotation speed of 2200 rpm.

Kumar et al. [10] examined the application of the FSW method in combining similar or different polymer materials and examined the mechanical, technical, and chemical properties of the materials. Using the Taguchi Experimental Design Method, they analyzed the effects of important processes and tool parameters on FSW of high-density polyethylene (HDPE) plate's weld strength [11].

Hamade et al. [12] conducted a feasibility and energy study showing the differences between the traditional Fusion Butt Welding (FBW) method and RFW method to join HDPE pipes, and conducted a cost analysis for both methods used in the study. In this cost analysis, it is shown that the energy consumption in RFW is one-tenth of the FBW. Kasman et al. [13] joined AA7075-T651 aluminum alloy sheets by friction stir welding method at two different rotation speeds using tools with 3 different pin geometries. Afterward, they compared the mechanical properties and microstructures of the welded areas.

If welded joints are to be tight and strong, some attention must be paid to the joint profiles. The strength of the weld should be at least as great as that of its two components, so that the area of the weld face must be about 2-2.5 times

the cross-section of the wall. V-profiles, used for many years now, has proved far the best; figure 2 shows two typical examples [14].
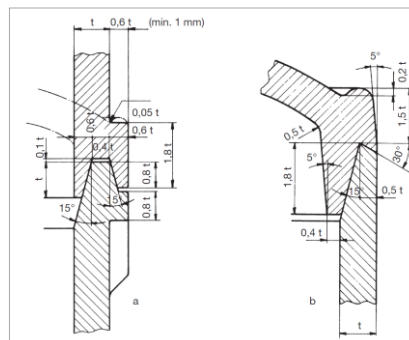

Figure 2. V profile joint profile [14]

D'Alvise et al. [15] produced a similar 2D coupled thermomechanical FE (Finite Element) model. The noticeable aspect of this model was that it underestimated the welding time and upset, but showed a good correlation with thermocouple data for the first 4 seconds of the welding process. Bennett et al. [16] produced a model using the commercial code Deform 2D attempting to fully simulate IFW (İnertia Friction Welding) by initially training the heating model using data from previously performed welds. This model considers the rotational motion by using a 2.5- dimensional element to model plane strain. Results of the upset prediction were only shown for the training phase of the model with an error of about 10%. Thermal profiles at 1 mm away from the final welding line were within 10% of the actual values, however further away from the weld line the difference increased.

Çevik et al. [17] investigated the weldability of high-density polyethylene materials by friction stir spot welding method. In their study, they observed that the pin length of the mixer set directly affects the welding quality.

In the literature reviews, it is observed that there are many studies on joining metal parts by RFW method, but there are very few studies on the use of this welding type on plastics. In this study, it is aimed to investigate the use of friction welding on polymer materials. RFW is used in joining of body and cover parts of many water purification filters. In this welding method, semi-melt agglomeration occurs in the inner and outer parts of the welding area. These accumulations can often cause clogging problems in the interiors of some sensitive filters. It is aimed to obtain a shape similar to the semi-melt agglomeration formed in the inner and outer parts of the filters with the ABAQUS program by Lagrangian and CEL (Coupled Eulerian-Lagrangian) methods. Several different joint profile designs that can confine the internal accumulation and prevent filters from clogging will be developed. It is aimed to find a more successful joint profile form by applying the analysis of these developed designs.

2. MELT AGGLOMERATION PROBLEM

Due to health reasons, many people use water purification devices in their houses and offices. These devices generally clean the water by passing it through separate filters. Filters of water purification devices consist of a body and a cover part made of polypropylene (PP) material. These parts are joined at their welding joint profile by RFW. Figure 3 shows this body and cover part. The welding joint profile design in this part is modeled according to the profile in figure 2.
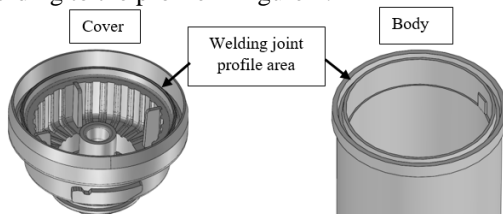
Figure 3. Body and cover part

After the rotary friction welding process, semi-melted agglomerations are formed on the inner areas of the body and cover parts. Figure 4 shows the welding joint profile design and semi-melted agglomeration after the body and
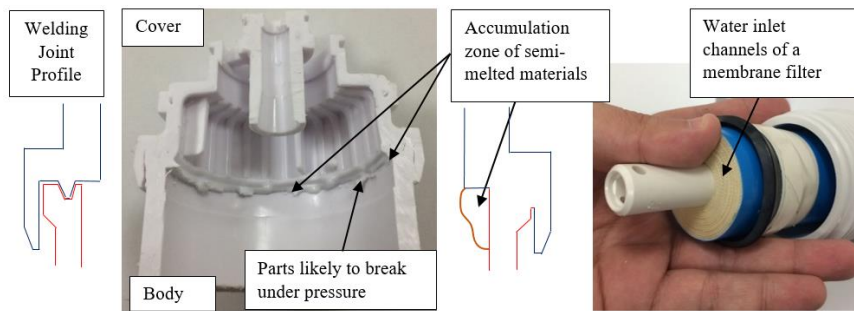
welding structures of these four filters and their semi-melted agglomerates

The proposed welding joint profile designs are shown in figure 5. Semi-melted agglomerations are observed on both inside and outside surfaces after the assemblies of these filters. The interior agglomeration growth is clearly visible in the figures. The accumulations formed on the outer surface of the filters (1), (2), and (3) can be cleaned using a lathe machine, however, post-weld cleaning in design number 4 is not necessary, due to the outer part geometry. It is seen that the welding joint profile structure of part (4) is similar to the proposed (figure 4) design. However, slight differences in terms of the part sizes can be mentioned resulting in varied agglomeration structures in the weld zone.

3. ANALYSIS OF FILTER WELDING JOİNT PROFİLE DESIGN

A FW machine starts the rotation process at the starting point, after reaching the desired rotation speed, it moves towards the body (with air pressure) and performs the friction welding process. While the cover part rotates and

Figure 4. Inline filter welding structure, accumulations in the inner and outer parts.

the cover piece are joined. Although the agglomeration is not important on the outer side, agglomerations in the inner side are important as ruptures may occur on these accumulations during the passage of pressurized water. Broken parts may cause clogging at water inlet channels of sensitive filters such as membrane filters.

moves downwards, the body part remains fixed to the base. Figure 6 shows the welding process of the filter in the FW machine used. After the welding machine completes the process, it stays for a while in the position where the process is finished and then returns to its starting position.
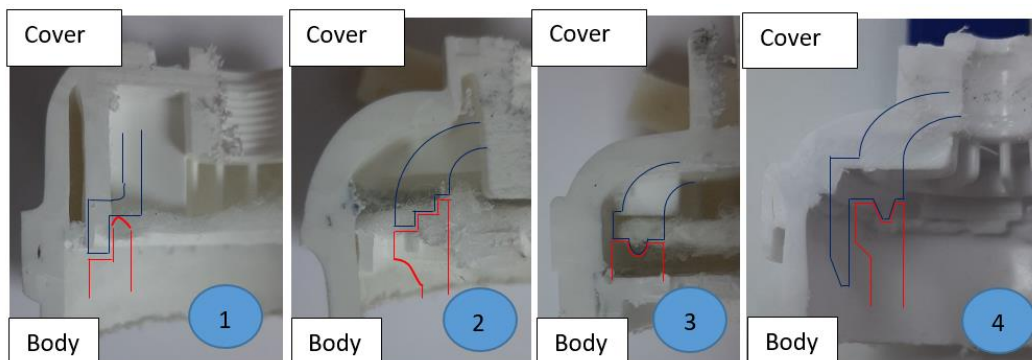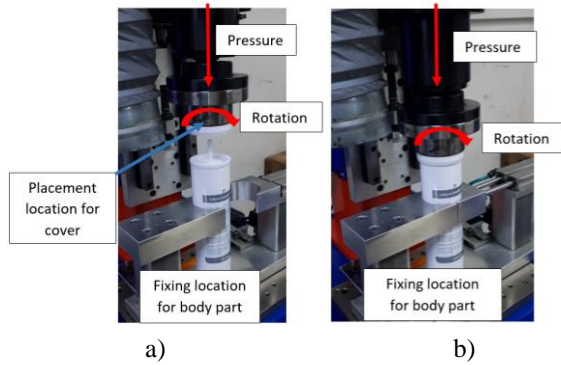
Figure 5. Welded parts of inline water filters

Filters of four different water purification systems available on the market are cut and examined in order to observe their post-weld structure. Figure 5 shows the

Figure 6. Friction welding machine starting position **a)** Friction welding machine welding process **b)**

The rotation speed entered into the machine before the welding process, the force applied during welding, the welding time, and the waiting time after welding throughout the experiment are shown in Table 1. The rotation process in the friction welding machine is provided by a servo motor. The process of making pressure on the part is done by an air pressure unit.

Table 1. Parameters entered in the friction welding machine

Input Parameter Name	Input Parameter Value
Rotation speed (rev / sec)	415
Friction welding pressure (bar)	6
Friction welding time (sec)	2
Friction waiting time after welding (sec)	3,5

The dimensions of the body and the cover are shown in figure 7 Actual parts are measured and the measurement values are used as input for ABAQUS software thus simulation variables are held as realistic as possible. In order to obtain realistic analysis results from an analyzing software, the operation sequence and data in the FW machine must be entered properly.
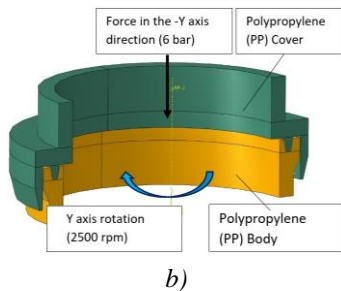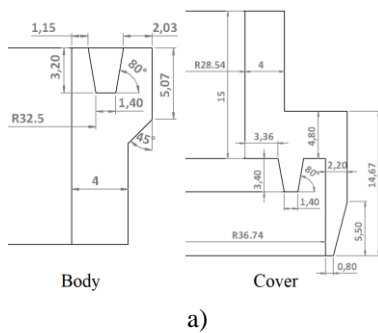

Figure 7. Dimensions of the part to be analyzed **a)** Part design modeled in ABAQUS **b)**

Polypropylene's basic material data which is required for the analysis of the body and cover parts in the ABAQUS program is shown in Table 2.

Table 2. Technical data of polypropylene [18]

	Test Method (ISO)	Value
Specific Weight (gr/cm³)	1183	0,92
Tensile Strength (MPa)	51,68	300
Elastic Modulus (MPa)	527	1250
Elongation at Break (%)	527	>50
Max. Continuous Working (°C)	-	100
Min. Continuous Working (°C)	-	5
Thermal Expansion Coefficient (°C⁻¹)	11359	$1,6 \times 10^{-4}$

In ABAQUS, fixing was made at the base of the body. The force was applied to the cover in the -y direction and rotational speed was given on the y-axis. For the friction welding solution of PP plastic material, firstly the transition part from solid to liquid state was analyzed with the Lagrangian method and then its behavior in the liquid state was analyzed with CEL (Coupled Eulerian-Lagrangian) element method. With the Lagrangian method, the analysis of the values under dynamic loads such as temperature, displacement, and stress over time was performed. In the analysis made by the Lagrangian method, the data of the body and cover parts from solid-state to liquid state were obtained. Figure 8 shows the analysis made with the Lagrangian method.
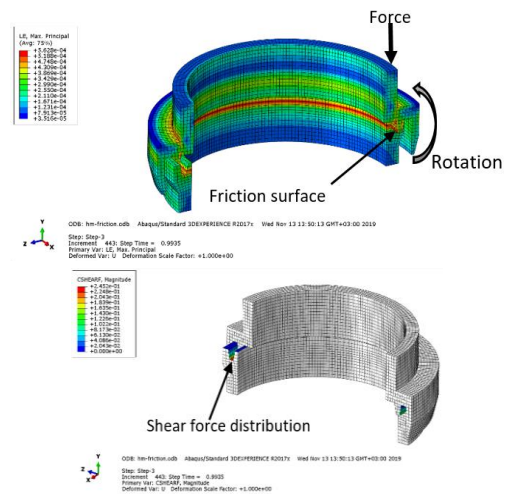

Figure 8. Analysis using the Langrangian method

When figure 8 is examined it is seen that, due to the design of the part, less rotation occurs towards the inner part when force is applied. Due to this rotation, more contact takes place in the inner region. This is the reason why the temperature inside is higher.

The data obtained from Langrangian analysis (such as centrifugal force, pressing force, reaction force formed inside the part) were applied on the part. These data were used as input data in the CEL method. The purpose of the CEL method is to obtain data such as temperature, force

distribution, state transitions in the melting state of the material. In order to observe the behavior of semi-melted material that has turned into a liquid from solid-state, an Eulerian part was designed in the weld area with the CEL method. Figure 9 shows the part and Eulerian designs made by the CEL method.
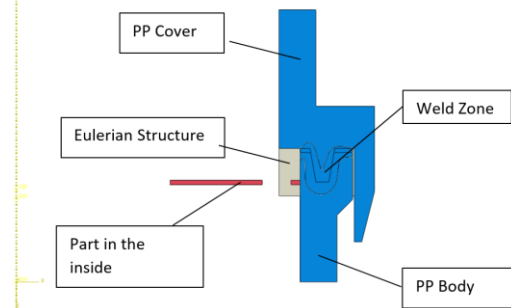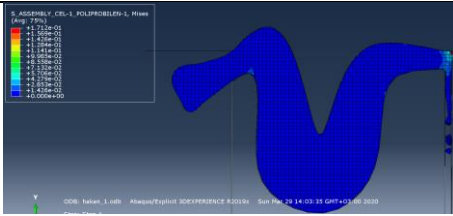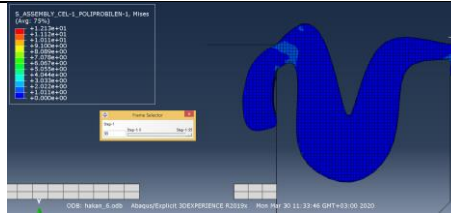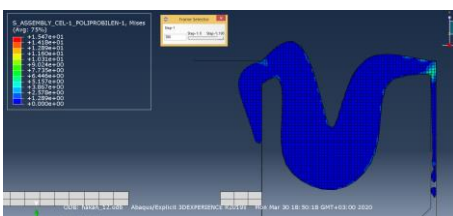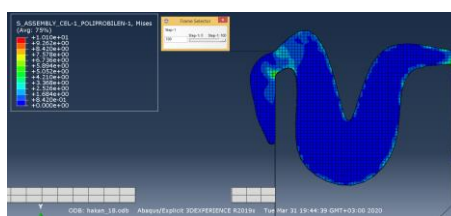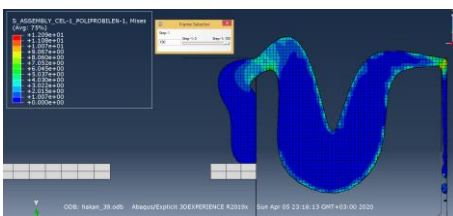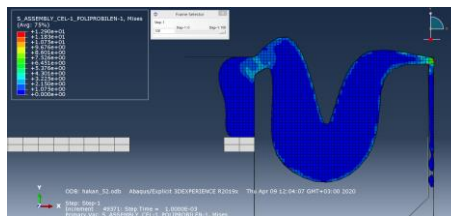

Figure 9. Design and part made in CEL method

After entering the data into the program and making necessary adjustments, the analysis phase was started. In the CEL analysis, adjustments were made without graphic options such as temperature, stress, energy, and displacement. By making adjustments in this way, the solution time of the analysis was reduced. In this way, it took about 6-8 hours to solve each analysis. If the graphs of stress, energy, and displacement were added, the analysis would take up to 5 days to resolve.
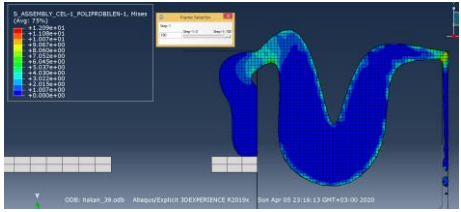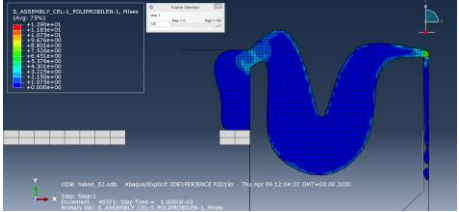
4. PHYSICAL-MECHANICAL ANALYSIS AND WELDING JOINT PROFILEDESIGN

Approximately 200 CEL analyzes were conducted on the program. Comparisons between semi-melted structures obtained from the results of this analysis and semi-melted agglomeration in figure 4 are made. The entered parameters changed and analyze repeated until the generated semi-melted agglomeration state resembles in figure 4. Some of these analyzes and their comments are given in Table 3

**Table 3.** Semi-melted state and comments after CEL analysis

While resolving this analysis, the program failed when the completion rate reached 87%. As seen in the analysis, the flow on the right is like water, and at the same time, an inward flow is observed on the left side. It is decided to make changes to the dynamic viscosity and radial force values.

In this analysis, it is seen that the flow is less on the right side, but the dynamic viscosity value is high and the radial force is low. It is considered to decrease the dynamic viscosity value and increase the EOS (Equation of State) value.

In this analysis, the high flow on the right indicates that the dynamic viscosity value is low. The radial force is close to the desired. Increasing the dynamic viscosity value is needed.

In this analysis, flow occurs on the right side, but it is evaluated that the dynamic viscosity and radial force values are close to the desired value. However, semi-melted agglomeration did not occur in the desired structure. An amendment in the Eulerian form is needed.

In this analysis, the high flow on the right side suggests that the dynamic viscosity value should be increased, and the gap on the left side suggests that the radial force should be increased. The semi-melted agglomeration is not in the desired structure as well.

The high flow on the right in this analysis suggests that the dynamic viscosity value should be increased. The radial force is close to the desired but the semi-melted agglomeration is not in the desired form. It is decided to amend the Eulerian form.

Table 3. (Continue) Semi-melted state and comments after CEL analysis

This analysis suggests that the dynamic viscosity value should be increased due to the high flow on the right side. The radial force is close to desired however the semi-melted agglomeration is not at the desired structure. A slight reduction of the EOS value is needed.

In this analysis, the flow on the right is at the desired level, so the desired dynamic viscosity value is reached. The radial force is also close to the desired value. The semi-melted agglomeration has the desired structure as well. It is decided to proceed to the next stages with the values used in this analysis.

The data entered into the software were changed to obtain semi-melted agglomeration close to the current model. It was determined that when the dynamic viscosity value is increased, the flow of semi-melted material slows down, and when it is lowered, the flow accelerates. It is seen that, in the semi-melted structure, when the radial force is increased, the inner semi-melted material flows more towards the outside, and when it is lowered, the material flows more towards the center. When the EOS value is entered too much, the material changes shape without compression, and when it is entered low, the material changes shape after a certain compression force is affected.
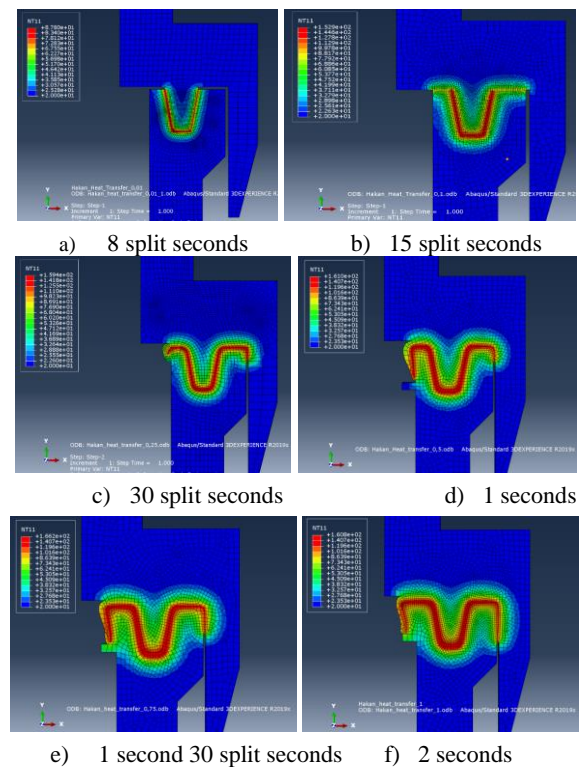
In figure 10, the semi-melted structure obtained in the CEL analysis is compared with the semi-melted agglomeration of the existing weld zone. It is seen that the structure obtained in the analysis is close to the existing structure.
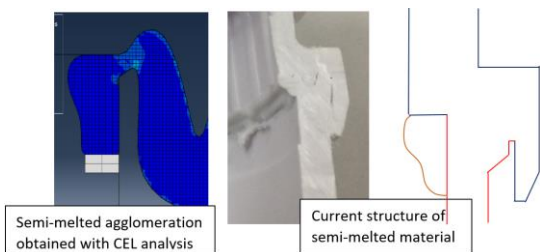
Figure 10. Comparison of the structure obtained from CEL analysis and the existing structure

4.1. Physical (Temperature) Analysis

According to the parameters that enable us to obtain the desired semi-melted structure, the temperature data of the part in the specified periods are defined. In order to obtain long-term analysis solutions, graphs were produced with a high capacity computer. Based on the analysis, temperature distribution, and structure of the part at a certain period of time can be seen in figure 11.

a) 8 split seconds   b) 15 split seconds

c) 30 split seconds   d) 1 seconds

e) 1 second 30 split seconds   f) 2 seconds

Figure 11. Temperature and semi-melted structure visuals according to time

After the contact begins between the parts, the pressure from the cover affects the interior. When looking at the 8th split second (figure 11a), it is seen that the temperature increases due to the greater friction pressure and surface contact in the interior of the piece. At the 15th split second (figure 11b), friction increases on all surfaces on the welding area. Consequently, the plastic in the welding joint profile began to melt. In the 30th split second (figure 11c), the plastic on all surfaces has become semi-melted and started to flow towards the inner and outer parts. While the flow of semi-melted material increased towards the inner side of the part in the 1st second (figure 11d), it is observed that there is not much flow to the outer part. Due to the outer protrusion and the narrow flow path, the flow of the semi-melted

material is slowed down and it is observed that it creates pressure towards the inner part. Therefore, it is determined that the semi-melted material flows more towards the inner part.

In the examination of the filter parts taken from the market, it was observed that the half-melted agglomeration occurred at equal densities in the inner and outer parts, due to the difference in the welding joint profile structures of the parts (1), (2), and (3) and because there were no walls on the outer parts to stop the flow. Half-melted agglomerates started to condense in the inner part between 1.5 seconds (figure 11e) and 2 seconds (figure 11f) and the plastic inside melts and flow over the previously solidified areas. For this reason, it was observed that the semi-melted material accumulation in the inner part increased and densified.

During welding, the temperature was measured with a Fluke remote temperature meter. During the measurement, the temperature on the part was observed to be 160.4 °C. The screenshot of the measurement is shown in figure 12.
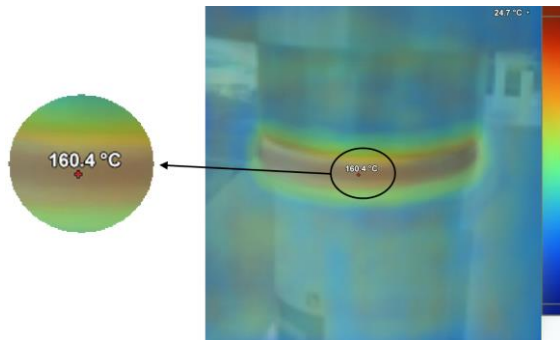

Figure 12. Temperature measurement during welding

After the welding process, the assembled part cools down by waiting 3.5 seconds on the machine. Figure 13 shows the heat distribution in the piece at the end of this waiting time. It is predicted that the maximum temperature of the part will be 98.4 ° C when the part leaves the welding machine.
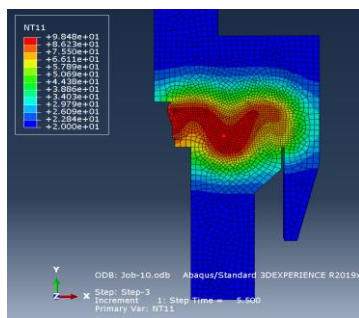

Figure 13. Heat distribution in the weld zone after 3.5 seconds

4.2. Mechanical (stress) Analysis

In figure 14, the stress on the part depending on the temperature is measured as 4.9253 MPa. It is observed that the stress value decreases as the material temperature increases. At the same time, part displacement is

determined depending on the temperature. When the analysis is completed, there is a 1.98 mm decrease in the -y direction in the length of the piece.
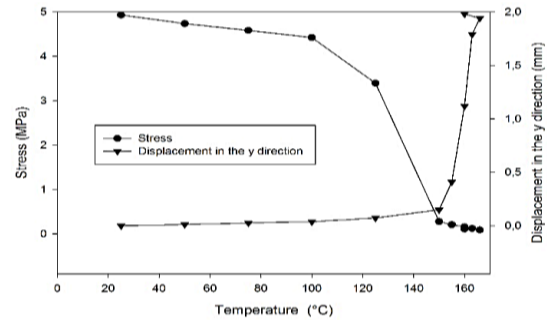

Figure 14. Displacement and stress chart

Figure 15 shows the graph of yield stress, Poisson's ratio, and modulus of elasticity depending on the temperature of the PP material. It is seen that the yield stress of the part increases when the plastic strain increases. While the yield stress is high at ambient temperature, the yield stress decreases as the temperature increases. Although the elasticity module decreases as the temperature increases, the Poisson's rate remains constant.
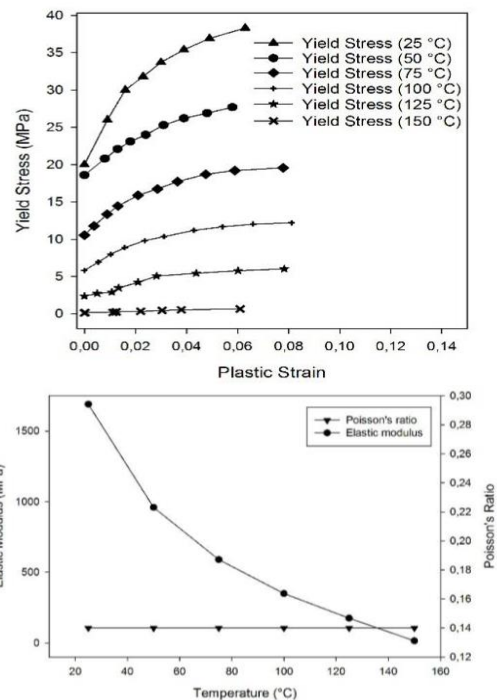
Figure 15. Temperature-dependent plastic strain, yield stress, Poisson's ratio, and elastic modulus graph

Figure 16 shows the graph of the temperature of the weld zone over time. In the analysis made, it is seen that the temperature in the weld zone reaches a maximum of 166.2 ° C and the material in the welding area reaches a temperature of 150 ° C in 13.1 split seconds. Due to the high speed and the pressure force, the welding area gets heated in a very short time.

Figure 16. Change of temperature according to time.

Figure 17 shows the Reaction Force Distribution in the y and x directions of the weld area of the cover piece. It is seen that the reacti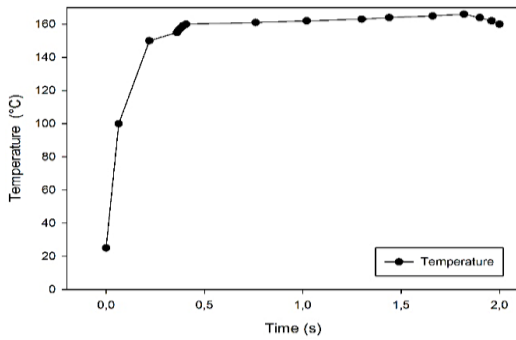on force in the -y direction affecting the cover piece increases with time and the force decreases towards the end of the welding. The reaction force in the -X direction increases in a fluctuating fashion according to the flow of the semi-melted material in the weld slot and decreases towards the end of the weld.
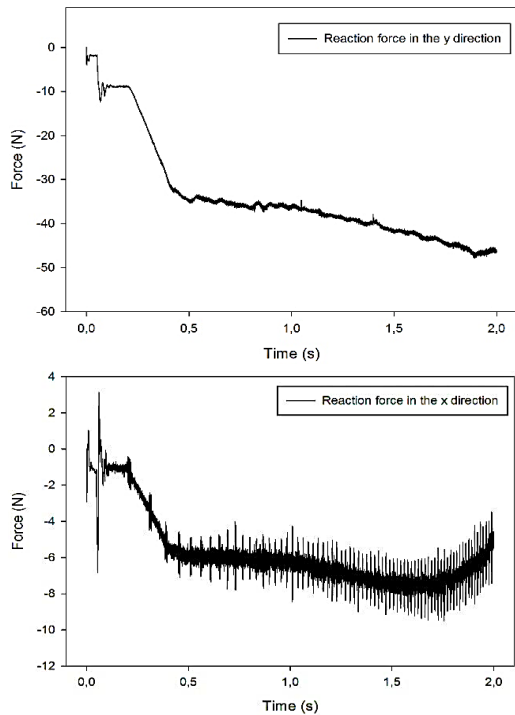

Figure 17. Reaction force graph on the cover part in x and y directions.

Figure 18 shows the reaction moment distribution affecting the weld area of the PP cover piece in the x and y direction relative to time. It is seen that the reaction moment force acting on the cover in the x direction increases with time. The reaction moment force in the Y direction increases in a fluctuating manner at the beginning and decreases afterward.
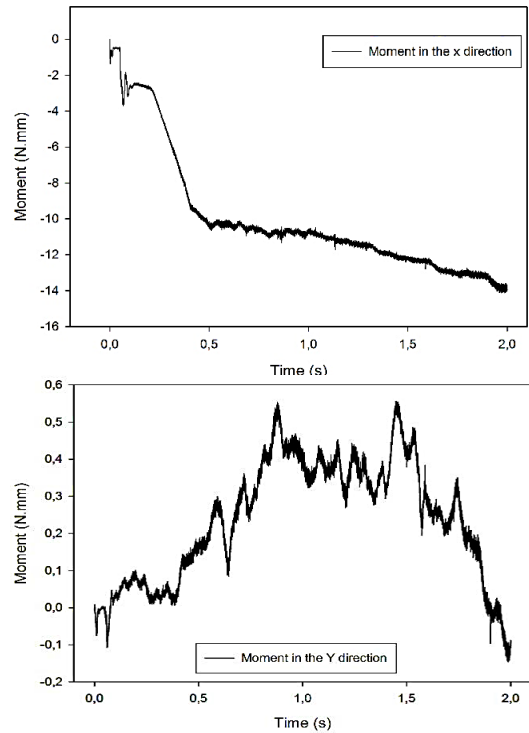
Figure 18. Reaction moment graph in x and y direction on the cover piece.

Figure 19 shows the time-dependent kinetic and internal energy graph in the welding area. At first, the kinetic energy appears to have a peak when the cover piece contacts the body. Then, the kinetic energy fluctuates relative to the time. While the amount of internal energy is small at first, its amount increases as the temperature increases, and the cover piece move in the -y direction.

Figure 19. Kinetic and internal energy in the part

The graph of the temperature-dependent friction coefficient of the PP material in the analyzes performed is shown in figure 20. As the temperature increases, the friction coefficient increases, and the temperature decreases when the melting point is reached.

Figure 20. PP friction coefficient chart

4.3. Welding Joint Profile Design

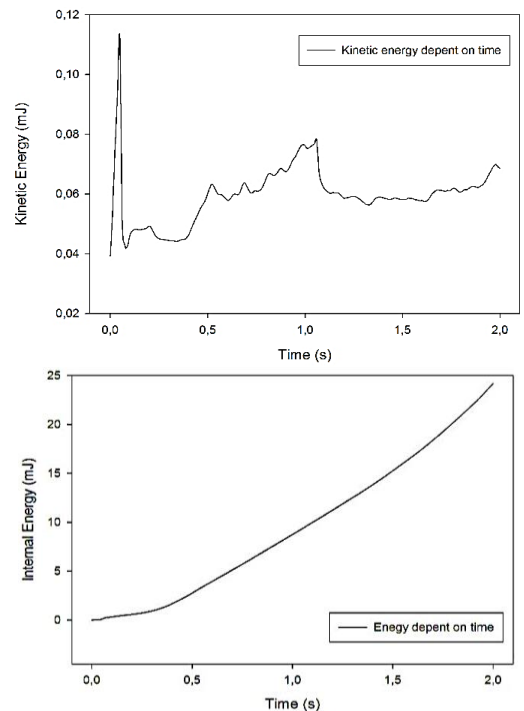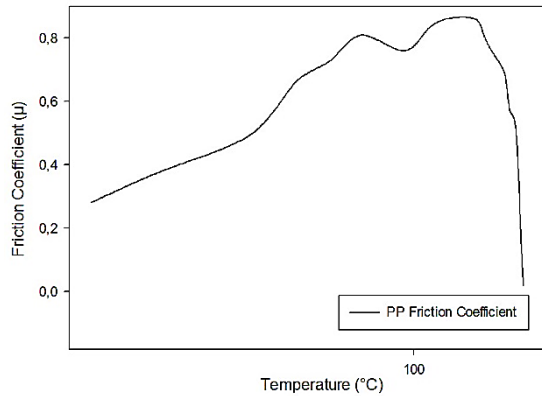After obtaining the existing semi-melted structure in the ABAQUS analysis program, the design of a weld joint profile preventing agglomeration in the interior surfaces is initiated according to the simulation output. Schmicker et al. [19] simulated RFW of metal parts in their own software program and in this simulation, they developed a weld joint profile design that traps semi-molten material inside during welding. In figure 21 below, the weld joint profile structure they developed and its post-welding state can be seen.
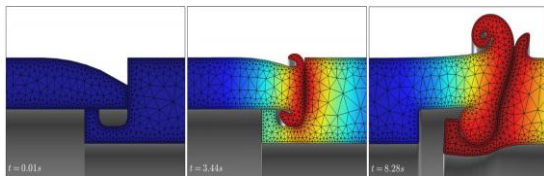
**Figure 21.** The agglomeration is trapped in the slot during the welding of metals [19]

Inspired by the design made by Schmicker et al., three different welding joint profile designs that can trap semi-molten agglomeration are developed. Figure 22 shows these developed welding joint profile designs.
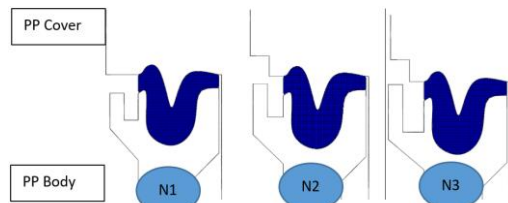
Figure 22. Welding joint profile structure designs

CEL analyzes for semi-melted agglomeration are performed for each of the newly developed weld joint profiles (namely N1, N2, and N3) using the data obtained from the previous analyzes. The results of the analysis are shown in figure 23.
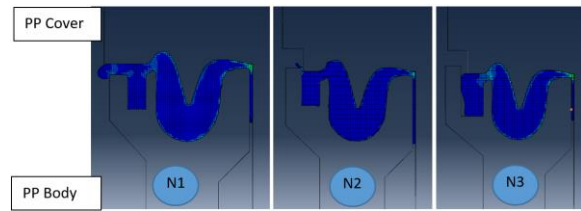
Figure 23. Results of CEL analysis of the weld component joints (N1), (N2), and (N3)

When the analysis of the design (N1) is examined, it is seen that the slot made for the confinement of the semi-melted agglomeration was insufficient. Semi-melted material filled the slot and overflowed.

Next, when the analysis made on the design numbered (N2) is examined, it is seen that the slot made to contain the semi-melted agglomeration is again insufficient. In this design, the semi-melted material filled the space and overflowed from the corner on the left side due to the increased pressure in the interior.

Finally, when the design numbered (N3) is analyzed, it is seen that the slot made to contain the semi-melted agglomeration is sufficient. The values in the analysis are stable in all conditions. However, since the values of a welding machine cannot be always stable, the depth and width measures in the design should be further optimized at the engineering stage.

5. RESULTS and DISCUSSIONS

Although many studies, simulations, and analyzes are done on joining metals by RFW method, there is not any remarkable study conducted on joining plastic materials. Kumar et al. [4] studied the mechanical and physical aspects of joining plastic parts by FW. Singh et al. [20] applied the Taguchi method to the input parameters of plastic parts that they reinforced with aluminum and iron powder. As a result of this study, they found that 775 rpm, 0.045 revs/mm, and 6 seconds welding time are the best parameter combination for aluminum powder reinforced plastics, and 1200 rpm, 0.045 revs/mm, and 8 seconds welding time are the best parameters combination for metal powder reinforced plastics.

Bindal et al. [21] joined the two PP materials by RFW and they analyzed the effects of welding pressure and rotational speed on this joint. The minimum distance value required to join the parts was measured as 64.1 kPa and 14.2 mm at 1100 rpm. Sahu et al. [22] performed experimental studies using the FSW method on 6 mm thick PP sheets. In these studies, it was observed that the conical pin could not join the thermoplastic materials. The square pin, on the other hand, successfully welded PP sheets, and they achieved a maximum welding strength efficiency of 59.82% in these welds. They observed that the feed and rotation speed of the tool is effective in obtaining high strength welds.

When the researches made on the joining of plastics are examined, no rotary friction welding simulations and analyzes are encountered. In this study, the analysis and simulations on RFW of plastic parts are made with the ABAQUS software.

The form of the semi-melted agglomeration in the body and cover parts of the water purification filters after RFW is simulated by the FEM (ABAQUS) program. Figure 24 shows the forms of agglomeration after rotary friction welding and the improved version of the weld joint profile design.
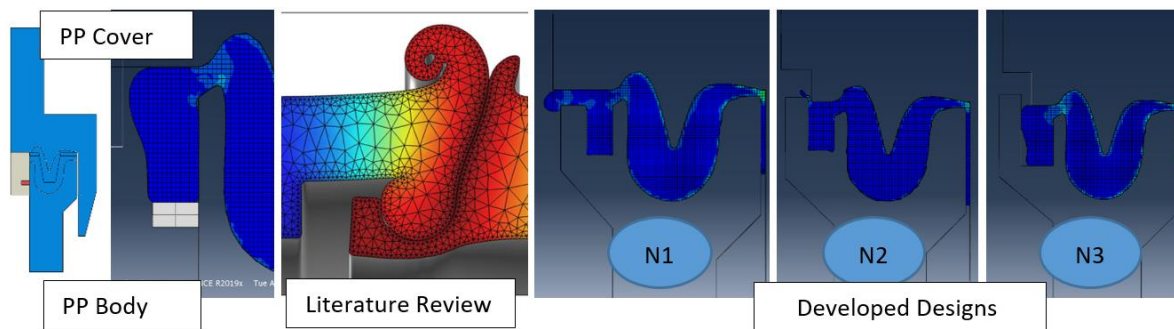
thermal profiles, stress distribution, and energy consumption graphs are pointed out as follows.

- It is observed from FEM analysis that the maximum temperature reaches 166.2 °C in the semi-melted material. Fluke device measure the maximum temperature as 160.4 ° C during the welding. As a result it seems that the FEM analysis and results of Fluke device measurements are similar to each other.
- According to the thermal analysis, a temperature

Figure 24. Semi-melted agglomeration after rotary friction welding

Part designs are carried out by utilizing ABAQUS software, and the parameters such as rotational speed and pressure in the FW machine are used as input data. The semi-melted agglomeration forms obtained as a result of the analyses are compared with the existing form and the most similar agglomeration form is determined. After obtaining the most suitable form, the graphs for thermal, stress, and energy are demonstrated.

Hamade et al. [23] combined high-density polyethylene materials with RFW at 1224 rpm rotation speed, 40 mm / min feed rate, 1085 N maximum thrust, and 13.5 sec welding time. They determined the maximum temperature as 250°C which is above the melting temperature of the material. In our study, the maximum temperature of the PP material is determined as 166.2 °C, which is also above the melting temperature of the material, at 2500 rpm, 6 bar pushing pressure, and 2 seconds welding time.

In the literature, various designs were proposed considering these kinds of undesired accumulations. Schmicker et al. [19] made a housing design to prevent accumulation on the inner surfaces of relevant metal assemblies during RFW. Inspired by this design, 3 different welding joint profile designs are proposed in this study. Semi-melted agglomeration distributions are obtained by applying CEL analysis to these designs. According to the results obtained, only design N3 traps semi-melted agglomeration as required.

6. CONCLUSION

In this study, the FEM (ABAQUS) program is utilized to obtain the desired semi-melted agglomeration form on a rotary-friction welded polypropylene filter. The resulting values obtained from this software considering the

of 150 ° C is reached in 13.1 split-seconds in the welding zone.

- After welding, there is a 1.98 mm shortening in the length of the part.
- The maximum stress value on the part is measured as 4.9253 MPa.
- The maximum temperature value of the final assembly removed from the welding machine is expected to be approximately 98.4 ° C.
- N3 numbered design is the most appropriate design with the best capability of semi-melted agglomeration confinement when compared with the other proposed designs in this study.

DECLARATION OF ETHICAL STANDARDS

The author(s) of this article declare that the materials and methods used in this study do not require ethical committee permission and/or legal-special permission.

AUTHORS' CONTRIBUTIONS

Hakan MADEN: Perofrmed the experiments, analyse the results and wrote the manuscript..

Kerim ÇETİNKAYA: Checked the analysis results.

CONFLICT OF INTEREST

There is no conflict of interest in this study.

REFERENCES

[1] Ertuğ, A., "Friction Welding", *Engineer and Mechanical Journal,* 21 (241) (1997).

[2] Tensi, H.M., Welz,w. Und Schwlam, M., "Temperaturen beim Reibschweipen von Aluminiumwerkstoffen", *München.* 58, 515-517, (1982).

[3] G·runauer, H, Gürleyik, M.Y., "Friction Welding of Casted Parts", *Journal of Engineering and Machine*, 30:357, (1989).

[4] Reiners, G. ve Kreye, H., Mikrostruktur und Mechanische Eigenshhaften von Reibschwebverbindungen aus Aluminuro und Stahl, **Schwei Ben und Schneiden Hamburg**, 40 H elf 3, (1988).

[5] Dede A., Soy A. and Aslanlar S., "Friction Welding Method", *SAU Journal Graduate School of Natural and Applied Engineering,* 6(1):7-12, (2002).

[6] Li W., Shi S., Wang F., Zhang Z., Ma T., and Li J., "Numerical Simulation of Friction Welding Processes Based on ABAQUS Environment", *Journal of Engineering Science and Technology Review,* 5 (3): 10-19, (2012).

[7] Kahraman B., "Joınıng Of 5754 Alumınıum Alloy Sheets, Used In The Automotıve Industry, Through Resıstance Spot Weldıng (Rsw) And Frıctıon Stır Spot Weldıng (Fssw*)", M. Sc. Thesis, Kocaeli University, Graduate School of Natural and Applied Engineering,* (2009).

[8] Yan, Y., Shen, Y., Lei, H., Zhuang, J. and Li, J., "Friction lap welding AA6061 alloy and GFR nylon: Influence of welding parameters and groove features on joint morphology and mechanical property", *Journal of Materials Processing Tech.,* 278, 116458, (2020).

[9] Xu X., You G., Ding Y., Tong X., Zai L. And Liu Q., "Microstructure and mechanical properties of inertia friction welded joints between high-strength low-alloy steel and medium carbon steel", *Journal of Materials Processing Tech.,* 286, 116811, 1-14, (2020).

[10] Kumar, R., Singh, R., Ahuja, I.P.S., Penna, R., and Feo, L., "Weldability of thermoplastic materials for friction stir welding- A state of art review and future applications", *Composites Part B,* 137:1–15, (2018).

[11] Ülker A., "Investıgatıon Of The Effects Of Weldıng Parameters On The Weld Strength In Frıctıon Stır Weldıng Of Hıgh Densıty Polyethylene Polymer Materıal And Optımızatıon Of Weldıng Parameters Wıth Taguchı Experımental Desıgn Method", *Ph. Thesis, Ege University, PhD. Thesis,* (2015).

[12] Hamade, R.F., Andari, T.R., Ammouri, A. H. and Jawahir, I.S., "Rotary Friction Welding versus Fusion Butt Welding of Plastic Pipes – Feasibility and Energy Perspective", *Procedia Manufacturing,* 33:693–700, (2019).

[13] Kasman Ş., Kahraman F., and Aydın A., "AA7075-T651 Assembled by Friction Stir Welding Method Investigation of the Effect of Different Mixer Pin Geometries of Aluminum Alloys on Welding Performance", *International Symposium on Innovative Technologies in Engineering and Science,* (2016).

[14] ESA-PSS-03-210, "Adhesive bonding handbook for advanced structural materials", *issue 2, Section 2, Page:91-144. Noordwijk : Eur. Space Agency, - 1 v,* (1995).

[15] L. D'Alvise, E. Massoni and S. Walle, "Finite element modeling of the inertia friction welding process between dissimilar materials", *J. Mater. Process. Tech.,* 125-126:387-391, (2002).

[16] Bennett C.J., Hyde T.H., Williams E.J., "Modeling and simulation of the inertia friction welding of shafts", *Proceedings of the Institution of Mechanical Engineers, Part L: Journal of Materials: Design and Applications,* 221(4):275–284, (2007).

[17] Çevik B., Gülenç B., and Durgutlu A., "The effects of critical welding parameters on tensile-shear properties of friction stir spot welded polyethylene", *Politeknik Dergisi,* 20(4): 945-951, (2017).

[18] Polypropylene properties, http://www.ozgunplastik.gen.tr/Polipropilen.htm Date of access: 12.011.2020

[19] Schmicker D., Persson P. O. And Strackelijan J., "Implicit Geometry Meshing for the simulation of Rotary Friction Welding", *Journal of Computational Physics,* 270:478-489, (2014).

[20] Singh R., Kumar R., Feo L., and Fraternali. F., "Friction welding of dissimilar plastic/polymer materials with metal powder reinforcement for engineering applications", *Composite Part B.,* 101:77-89, (2016).

[21] Bindal T., Saxena R. K., Pandey S., "Analysis of joint overlap during friction spin welding of plastics", *Materials Today: Proceedings,* 26:2798–2804, (2020).

[22] Sahu S. K., Mishra D., Mahto R. P., Sharma V. M., Pal S. K., Pal K., Banerjee S., Dash P., "Friction stir welding of polypropylene sheet", *Engineering Science and Technology, an International Journal,* 21:245–254, (2018).

[23] Hamade R. F., Andari T. R., Ammouri A. H., and Jawahir I. S., "Rotary Friction Welding versus Fusion Butt Welding of Plastic Pipes – Feasibility and Energy Perspective", *Procedia Manufacturing,* 33:693–700, (2019).